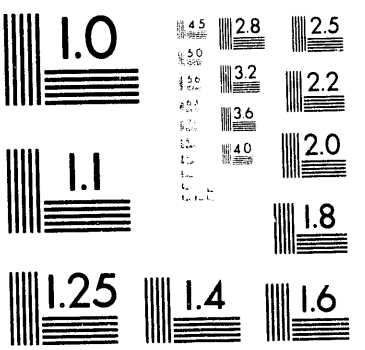
1.0
1.1
1.25
1.4
1.6
1.8
2.0
2.2
2.5
2.8
3.2
3.6
4.0
4.5
5.0

1 of 1

58906-00-105
85088-20-105
INVITED PAPER
August 1993

The Effect of Correlated and Point Defects on the Vortex Lattice Melting Transition in Single Crystal $YBa_2Cu_3O_{7-\delta}$*

W.K. Kwok,[a] J. Fendrich,[a,b] S. Fleshler,[a] U. Welp,[a]
J. Downey,[a] and G.W. Crabtree,[a] and J. Giapintzakis[c]

[a]*Materials Science Division and Science & Technology Center for Superconductivity Argonne National Laboratory, Argonne, Illinois 60439*

[b]*Department of Physics and Astronomy, Iowa State University, Ames, IA 50011*

[c]*Department of Physics and Materials Research Laboratory and Science & Technology Center for Superconductivity, University of Illinois at Urbana, Urbana, IL 61801*

*Work supported by the U.S. Department of Energy, BES-Materials Sciences under contract #W-31-109-ENG-38 (WKK, JF, SF, JD, GWC), the National Science Foundation--Office of Science and Technology Centers under contract #DMR 91-20000 (UW, JG).

Invited Talk: Proceedings of the XX International Conference on Low Temperature Physics, August 4-11, 1993, Eugene, OR.

The effect of correlated and point defects on the vortex lattice melting transition in single crystal $YBa_2Cu_3O_{7-\delta}$

W. K. Kwok[a], J. Fendrich[a,b], S. Fleshler[a], U. Welp[a], J. Downey[a], G. W. Crabtree[a] and J. Giapintzakis[c]

[a]Materials Science Division and Science and Technology Center for Superconductivity, Argonne National Laboratory, 9700 S. Cass Ave., Argonne, Illinois 60439, U. S. A.
[b]Department of Physics and Astronomy, Iowa State University, Ames, Iowa 50011, U. S. A.
[c]Department of Physics and Materials Research Laboratory and Science and Technology Center for Superconductivity, University of Illinois at Urbana-Champaign, 1110 West Green Street, Urbana, Illinois 61801, U. S. A.

PACS: 74., 72., 61.80.-x, 05.70.Fh

ABSTRACT

The vortex melting transition T_m in several untwinned and twinned crystals is measured resistively in fields up to 8 Tesla. A Lindemann criterion for vortex lattice melting is obtained in addition to a sharp hysteresis in the magnetoresistance at B_m supporting a first order phase transition. The anisotropy of twin boundary pinning and its reduction of the "kink" in $\rho(T)$ associated with the first order melting transition is discussed in samples with very dilute twin boundaries. We also report on the direct suppression of the melting transition by intrinsic pinning for H || ab and by electron- irradiation-induced point defects.

Proceedings of the XX International Conference in Low Temperature Physics August 4-11, 1993, Eugene, Oregon, U. S. A. (INVITED TALK).

The effect of correlated and point defects on the vortex lattice melting transition in single crystal $YBa_2Cu_3O_{7-\delta}$

W. K. Kwok[a], J. Fendrich[a,b], S. Fleshler[a], U. Welp[a], J. Downey[a], G. W. Crabtree[a] and J. Giapintzakis[c]

[a]Materials Science Division and Science and Technology Center for Superconductivity, Argonne National Laboratory, 9700 S. Cass Ave., Argonne, Illinois 60439, U. S. A.
[b]Department of Physics and Astronomy, Iowa State University, Ames, Iowa 50011, U. S. A.
[c]Department of Physics and Materials Research Laboratory and Science and Technology Center for Superconductivity, University of Illinois at Urbana-Champaign, 1110 West Green Street, Urbana, Illinois 61801, U. S. A.

PACS: 74., 72., 61.80.-x, 05.70.Fh

Abstract

The vortex melting transition T_m in several untwinned and twinned crystals is measured resistively in fields up to 8 Tesla. A Lindemann criterion for vortex lattice melting is obtained in addition to a sharp hysteresis in the magnetoresistance at B_m supporting a first order phase transition. The anisotropy of twin boundary pinning and its reduction of the "kink" in $\rho(T)$ associated with the first order melting transition is discussed in samples with very dilute twin boundaries. We also report on the direct suppression of the melting transition by intrinsic pinning for H || ab and by electron- irradiation-induced point defects.

1. Introduction

Recent experiments have shown support for a first order vortex melting transition at T_m in high quality untwinned single crystals of $YBa_2Cu_3O_{7-\delta}$ [1-5]. One of the strong supporting evidences for such a transition is the hysteresis observed in the temperature and field dependence of the resistivity $\rho(T,H)$ as reported by Safar et al. using pico-volt sensitivity measurements [1]. In this manuscript we show with conventional electronics, an extremely sharp transition of $\rho(H)$ at T_m, in addition to a pronounced asymmetric hysteresis loop. The width of the transition $\rho(H)$ at T_m of the decreasing magnetic field branch of the hysteresis loop for $H \parallel c$ is less than 10 Oe in a field of H~6Tesla. This suggests that the sharp drop in $\rho(H)$ at T_m is indeed a first order melting transition. In the same crystal, we obtain a reasonable Lindemann criterion for melting determined from a fit to the angular dependence of $T_m(\theta)$. Furthermore, in dilutely twinned crystals, we show directly that the magnitude of the "kink" in the magnetoresistivity associated with the first order vortex melting transition at T_m is reduced but not destroyed in the presence of a few twin boundaries. However, in the presence of increased point defects induced by electron irradiation on an untwinned crystal, we show that the first order melting transition is replaced by a second order transition T_g at lower temperature. A similar behavior is observed in the presence of intrinsic pinning, however, the nature of the second order transition for this geometry is reminiscent of the continuous nematic to smectic transition found in liquid crystals.

2. Experiment

Five single crystals of $YBa_2Cu_3O_{7-\delta}$ were grown by the self-flux method described elsewhere [6] and displayed $T_c > 92.0K$ with transition width $\Delta T <$

300mK. Crystal A is an untwinned sample, de-twinned by applying uni-axial pressure along one of its crystallographic a/b axis [7]. Crystal B is an as- grown crystal containing only a single twin boundary. Crystal C is another de-twinned crystal prepared such that only six twin boundaries remained as determined by polarized light microscopy. Finally, crystal D is a de-twinned crystal which was irradiated with 1Mev electrons at 35K. Table 1 shows the characteristic temperatures and features of each crystal. AC resistivity measurements were done by the standard four probe method with a typical measuring current density of $j \sim 0.3 A/cm^2$ at 17 Hz, directed in the ab-plane of the crystal. Voltage-current characteristics were measured by the dc method by reversing the current flow at each current value to minimize thermal voltages. The sample was placed in the bore of two orthogonal superconducting magnets which delivered a longitudinal field of up to 8 Tesla and a maximum transverse field of 1.5 Tesla. By computer control of the two magnets, the resultant field could be accurately rotated about a crystal axis with an extremely high precision $\Delta\theta < 0.001^o$ [8].

3. Results and discussion

3.1 Vortex melting transition

Figure 1 shows the temperature dependence of the resistivity in fields up to 8 Tesla for both H | | c and H | | ab orientations of Crystal A.
The magnetic field is always perpendicular to the measuring current in the ab-plane. For both geometries, a very sharp "kink" in the resistivity is observed near the tail of the resistive transition. The width of the "kink" is extremely small, and at 4T | | c, ΔT_{kink}(10-90%)~50mK, much less than the zero field transition width of ΔT_c(10-

90%)~200mK. At intermediate and low fields, ie. H<7T, and for H || c, the "kink" separates the regime between ohmic behavior at temperatures above the "kink" and non-ohmic behavior for temperatures below it [1,4,5,9]. At higher fields, the temperature width of the "kink" becomes broader and ohmic behavior is sustained down to the tail of the resistive transition. The broadening of the "kink" has been related to increased disorder at high fields [10]. Another interesting feature of the "kink" is that its resistive magnitude is virtually constant as a function of the magnitude and direction of the magnetic field for temperatures about 1.5 K below T_c.

Figure 2 shows the field dependence of the resistivity $\rho(H)$ at T=81.386K for H || c. The arrows show the increasing and decreasing magnetic field sweeps. We find the increasing field transition curve to be broader than the decreasing field transition curve which in this case is extremely narrow and always occurs at lower magnetic fields. The width of the decreasing field transition curve is $\Delta H<10$ Oe at B_m=5.87 Tesla which translates to one part in 10^4! The hysteresis loop width is about 200 Oe, determined at the midpoint of the increasing and decreasing field curves. This strongly suggests that the vortex melting transition at B_m is of first order. The hysteresis loop shows that for a constant temperature, the melting field is higher than the solidification field. This may be explained by the dynamic behavior of the glassy state. Geshkenbein et al. [11] have argued that upon decreasing the magnetic field from the liquid state, the vortex liquid freezes into a solid state at B_m due to the existence of quenched random point disorder which destroys the long range order of the Abrikosov lattice. However, due to the broad distribution of relaxation times in the glass state, the equilibrium state of the glass is never achieved and its free energy slowly relaxes to lower values with time. Thus upon increasing the magnetic field, the free energy is now lower than the free energy of the liquid, and the transition

which occurred at B_m occurs at a higher field. The asymmetry of the hysteresis loop can be explained as follows. For a fixed field and at temperatures below T_m, the vortices are in the glassy state. With increasing magnetic field, the vortices may melt inhomogeneously in domains, each domain choosing a melting field appropriate to the balance between thermal, vortex interaction, and pinning energies for its local defect pattern. This accounts for the broad width in $\rho(H)$ at the melting transition for increasing magnetic fields. However, in decreasing the field from the vortex liquid state, if the vortex-vortex interaction is greater than the vortex-pin site interaction, which may well be the case for clean untwinned crystals, the vortices are more likely to freeze homogeneously into a large Abrikosov lattice domain, giving an extremely sharp single transition upon freezing. At lower temperatures, this domain will break up into smaller Larkin domains due to the increased strength of random point pinning disorder [11].

The H-T phase diagram obtained by taking the derivative of the curves in Fig. 1 and determining T_m from the peak in $d\rho(T)/dT$ at the "kink" is shown in figure 3. The curves exhibit a power law behavior $H \sim H_o(T_c - T_m)^n$ with n=1.46 and 1.45 respectively for H | | c and H | | ab. The mass anisotropy can be obtained from the ratio of the pre-factors and yields $\Gamma = \sqrt{M/m} = 8.7$. We determined the Lindemann criterion from the angular dependence of T_m obtained by monitoring the "kink" temperature from the $\rho(T)$ curves for H=1.5T at various angles of the magnetic field between the c-axis and the ab-plane of the crystal. The results are shown in Fig. 4 where we fit our data to the following equation for $T_m(\theta)$ [3, 13] using the two fluid model for the penetration depth $\lambda(T)$, and $\varepsilon = (\sin^2\theta + \Gamma^2\cos^2\theta)$ is the magnetic field scaling parameter.

$$k_B T_m = \frac{\Phi_o^{5/2} c_L^2}{4\pi^2 \lambda^2 (T_m) B^{1/2} \varepsilon^{1/4} (\theta)} \qquad (1)$$

Using Γ=8.7 and λ(T=0)=1400Å, we obtain the best fit with T_c=93.4K, which yields a reasonable Lindemann criterion of c_L=0.17.

Now that we have established the first order nature of the vortex melting transition at T_m, we proceed to determine the effect of disorder on the melting transition.

3.2 Effect of twin boundary pinning on T_m

Imry and Wortis [14] have predicted the smearing of a first order phase transition in the presence of a finite density of defects. With increasing defects, the first order phase transition may be replaced by a second order transition. Our previous investigations of twin boundary pinning in $YBa_2Cu_3O_{7-\delta}$ suggests that twin boundaries, with various orientations with respect to the current induced Lorentz force may provide an ideal situation to investigate the effect of pinning on the vortex melting transition [4,15].

Figure 5 shows the resistive transition in a magnetic field of 4T $\|$ c for Crystal B containing only a single twin boundary oriented at 90 degrees with respect to the measuring current. The inset shows the dramatic effect of single twin boundary pinning as a function of tilt angle off the c-axis and towards the ab-plane. Our earlier results have shown that in this geometry where the Lorentz force is oriented parallel to the twin boundaries, the latter act as weak point pinning centers [15], since the vortices do not have to cross a two dimensional strain field and instead, are merely pinned weakly by point defects within a twin boundary. At

T_{TB}=85.09K, we see a weak shoulder related to the onset of twin boundary pinning. At lower temperatures, we still observe the sharp drop in resistivity at the melting transition T_m. Also shown is a curve with a measuring current of 1.0mA. The "kink" clearly separates the ohmic from the non-ohmic regime.

We can increase the effect of twin boundary pinning in two ways, either by increasing the number of twin boundaries or orienting the current induced Lorentz force direction such that the vortices are forced to cross a strain field [15]. Figure 6 shows the resistive transition in a field of 6 Tesla for Crystal C which contains only six twin boundaries oriented at 45 degrees with respect to the measuring current such that the induced Lorentz force is at 45 degrees with respect to the two dimensional strain field of the twin boundaries. For $\theta=0^o$ where θ is the tilt angle between the magnetic field and the c-axis, we observe a pronounced shoulder at T_{TB} due to the onset of twin boundary pinning. At lower temperatures, for the same curve, a reduced "kink" is observed at T_m. In order to verify that the "kink" is of the same origin as the vortex melting transition discussed above, we tilted the magnetic field by 1.2 degrees off the c-axis. The tilted magnetic field reduces the effect of twin boundary pinning on the vortices as shown by the inset in Fig. 6 where the angular dependence of the resistance at fixed temperature and field shows a sharp dip at $\theta=0^o$ (ie. H || c || TB) with width $\Delta\theta\sim1^o$. Thus with $\theta=1.2^o$, we recover the full resistive height of the vortex melting "kink". Furthermore, Fig. 7 shows the hysteresis in the field dependence of the resistivity near the "kink" temperature for $\theta=1.2^o$ and T=79.01K. Compared with figure 2, the decreasing branch of the magnetoresistance curve is not as sharp, perhaps due to pinning in the vortex liquid state which reduces the height of the "kink" associated with the first order transition and also induces inhomogeneous freezing upon approaching T_m from above. The

reduction of the "kink" height may be brought about by the increased pinning of the vortex liquid with the underlying pinning site. For Crystal B with only one twin boundary, only vortices near the twin boundary will be affected whereas the majority of the vortices on either side of the twin boundary are free to slide. In contrast, all the vortices will be affected by the twin boundary in Crystal C due to the orientation of the Lorentz force with respect to the twin boundary. Thus we see a greater height reduction of $\rho(T_m)$ for the latter crystal. Another mechanism which may be responsible for the drop in resistivity besides vortex liquid pinning is topological vortex entanglement induced by the twin boundaries. This vortex-vortex interaction is predicted to allow for a few macroscopic defects to pin a large number of vortices [16].

3.3 Effect of point defects on T_m

In order to investigate the effect of random point defects on the vortex melting transition, we irradiated a de-twinned single crystal (Crystal D) with a fluence of $\Phi=1x10^{-19}cm^2$ of 1 MeV electrons at 35K. Assuming the induced defects are limited to the CuO_2 planes and setting the threshold energy for displacement equal to the measured maximum recoil energy for producing a defect, the cross sections for collision can be calculated [17]. We estimate a total defect density of approximately $3.64 \times 10^{13}/cm^3$ for Cu and $4.56 \times 10^{12}/cm^3$ for O in our crystal. After electron irradiation, we observe a slight depression of the zero field superconducting resistive transition from 93.16K to 92.08K and a slight increase in the normal state resistivity from $\rho(100K)= 122\ \mu\Omega$-cm to $128\ \mu\Omega$-cm. The resistive transition for H=4T $\|$ c is shown in Fig. 8 with normalized resistivity and temperature, before and after electron irradiation. Clearly, the "kink" at T_m is

completely suppressed after irradiation and is replaced by a smooth curve with zero resistance occurring at a lower temperature. Before irradiation, the "kink" at T_m separated the ohmic regime from the non-ohmic regime. After irradiation, we find an ohmic regime down to the nominal zero resistance temperature, and non-ohmicity is found at a much lower temperature.

The voltage-current (I-V) characteristics are shown in Fig. 9. Before electron irradiation, the I-V curves show ohmic behavior above the resistive "kink" at Tm and non-ohmic behavior below the "kink" as shown in the upper panel of Fig. 9. Just below the "kink" temperature we observe an S-shaped I-V curve. The S-shape separates the thermally activated flux flow behavior of the vortex solid at low current densities from the free flux flow of the vortex solid at higher current densities. After electron irradiation, we observe the ohmic regime to extend down to much lower temperatures. Furthermore, the S-shape behavior is no longer observed even in the non-ohmic regime below T/T_c=0.8817. This implies that the vortex liquid regime is pushed down to lower temperatures in the presence of defects. In other words, the irreversibility line, defined as the temperature where non-ohmicity occurs and hence a true critical current is observed, is lowered by electron irradiation.

3.4 Effect of intrinsic pinning on T_m

So far we have investigated the effect of random pin sites in the form of point defects introduced by electron irradiation and two dimensional correlated defects in the form of twin boundaries on the first order melting transition. Another interesting and very different type of pin sites come from the natural layered structure of the material which leads to a modulation of the superconducting order parameter along the crystallographic c-axis. This periodic pinning structure leads to the effect of

intrinsic pinning first introduced by Tachiki and Takahashi [18] where at low temperatures, the vortices will tend to localize between the double CuO_2 planes in $YBa_2Cu_3O_{7-\delta}$ in order to take advantage of the lower condensation energy. We have shown earlier that even at high temperatures where the vortex coherence length is larger than the layer spacing, the vortices can still be pinned by the 'washboard' potential coming from the modulation of the order parameter along the c-axis [8]. To investigate the effect of intrinsic pinning on melting, we applied the magnetic field parallel to the ab-plane of Crystal C.

Figure 10 shows the tail of the resistive transition in a magnetic field of 8 Tesla misaligned from the ab-plane by a small angle θ. The "kink" at T_m for finite $\theta \neq 0$ is similar to the one shown in the bottom panel of Fig. 1. Orientation of the magnetic field towards the ab-plane causes the resistive height of the "kink" to diminish, until at $\theta = 0^o$ ($H \| ab$), the "kink" is virtually absent and is replaced with a smooth featureless curve down to zero resistance. Assuming that intrinsic pinning has replaced the first order phase transition at T_m with a continuous second order transition at a lower temperature T^*, we can fit the resistivity curve to $\rho \sim (T-T^*)^s$ in order to extract a dynamic scaling exponent s.

Figure 11 shows a plot of $1/[(1/\rho)(d\rho/dT)]$ versus T for H=6T. We fit a linear curve to the tail of the resistive transition in the ohmic regime between the onset of intrinsic pinning at T=91.5K and the beginning of the non-ohmic regime at T=90.7K in order to extract s and T^*.

The extracted values of s at several fields are shown in the inset of Fig. 12. s is virtually field independent and centered at s=1.35. This value is much smaller than the values of 6.5 and 4 associated with the vortex glass [19] and Bose glass [20] models. For $H \| ab$, the uniaxial anisotropy of the superconducting order parameter

leads to a distorted hexagonal vortex structure inducing bond orientational order in the vortex state similar to the nematic state in liquid crystals. The periodic pinning potential induced by intrinsic pinning opens the possibility of inducing a one dimensional vortex density wave along the c-axis with translational periodicity related to the layer spacing, somewhat similar to the smectic phase of liquid crystals [21]. Thus near the onset of intrinsic pinning where the curves for $\theta=0.5^{o}$ and 0^{o} deviate from each other, a short range smectic ordering of the vortices may begin to develop. However, due to thermal fluctuations, the second order phase transition from the nematic to smectic vortex phase is shifted to lower temperatures at T^{*}. Figure 12 shows the H-T* phase diagram obtained from the T* values extracted from fits like those in Fig. 11. A power law fit to the data yields $H(T^{*})=1.70(T_{c}-T^{*})^{1.28}$.

4. Conclusion

We have shown that an intrinsic first order melting transition of the vortex solid exists in high quality twinned and untwinned single crystals of $YBa_2Cu_3O_{7-\delta}$. In the presence of dilute twin boundaries, the sharp "kink" in the magnetoresistivity associated with the first order transition may be slightly broadened in temperature and field, and its magnitude reduced considerably. We speculate that the reduction of the "kink" height may be due to increased interaction between the vortices in the liquid state and the twin boundaries which leads to a larger friction component. In addition, vortex entanglement near the twin boundaries which increases the viscosity in the vortex liquid state may also lead to a reduction of the resistivity above the melting temperature T_m. In the case of increased random point pinning sites, induced by electron irradiation, we find that the first order melting transition is replaced by a second order continuous melting transition at lower temperatures.

This shows directly that the first order phase transition cannot be sustained in the presence of a high density of disorder. Finally, for the case of intrinsic pinning for vortices parallel to the ab-plane, we find that the first order transition at T_m is replaced by a continuous second order transition at lower temperature T^*, reminiscent of the nematic-smectic transition in liquid crystals.

Acknowledgments

This work was supported by the U. S. Department of Energy, BES--Materials Science under contract #W-31-109-ENG-38 (WKK, JF, SF, JD, GWC) and the NSF-Office of Science and Technology Centers under contract #STC91-20000 (UW, JG) Science and Technology Center for Superconductivity.

References

[1] H. Safar, P. L. Gammel, D. A. Huse, and D. J. Bishop, Phys. Rev. Lett. 69, 824 (1992).

[2] D. E. Farrell, J. P. Rice, and D. M. Ginsberg, Phys. Rev. Lett. 67, 1165 (1991).

[3] R. G. Beck, D. E. Farrell, J. P. Rice, D. M. Ginsberg, and V. G. Kogan, Phys. Rev. Lett. 68, 1594 (1992).

[4] W. K. Kwok, S. Fleshler, U. Welp, V. M. Vinokur, J. Downey, G. W. Crabtree, and M. M. Miller, Phys. Rev. Lett. 69, 3370 (1992).

[5] M. Charalambous, J. Chaussy, and P. Lejay, Phys. Rev. B45, 5091 (1992).

[6] D. L. Kaiser, F. Holtzberg, M. F. Chisholm, T. K. Worthington, J. Cryst. Growth 85, 593 (1987).

[7] U. Welp, M. Grimsditch, H. You, W. K. Kwok, M. M. Fang, G. W. Crabtree and J. Z. Liu, Physica C161, 1 (1989).

[8] W. K. Kwok, U. Welp, V. M. Vinokur, S Fleshler, J. Downey, and G. W. Crabtree, Phys. Rev. Lett. 67, 390 (1991).

[9] W. K. Kwok, U. Welp, G. W> Crabtree, K. G. Vandervoort, R. Hulscher, and J. Z. Liu, Phys. Rev. Lett. 64, 966 (1990).

[10] H. Safar, P. L. Gammel, D. A. Huse, D. J. Bishop, W. C. Lee, J. Giapintzakis, and D. M. Ginsberg, Phys. Rev. Lett. 70, 3800 (1993).

[11] V. B. Geshkenbein, I. B. Ioffe and A. I. Larkin, pre-print (1993).

[12] A. I. Larkin, Sov. Phys. JETP 31, 784 (1970).

[13] G. Blatter, V. B. Geshkenbein, and A. I. Larkin, Phys. Rev. Lett. 68, 875 (1992).

[14] Y. Imry and M. Wortis, Phys. Rev. B19, 3580 (1979).

[15] S. Fleshler , W. K. Kwok, U. Welp, V. M. Vinokur, M. K. Smith, J. Downey, and G. W. Crabtree, Phys. Rev. B47, 14448 (1993).

[16] M. Cristina Marchetti and David R. Nelson, Phys. Rev. B42, 9938 (1990).

[17] J. Giapintzakis, W. C. Lee, J. P. Rice, D. M. Ginsberg, I. M. Robertson, R. Wheeler, M. A. Kirk, and M. -O. Ruault, Phys. Rev. B45, 10677 (1992).

[18] M. Tachiki and S. Takahashi, Solid State Commun. 70, 291 (1989).

[19] D. S. Fisher, M. P. A. Fisher, and D. A. Huse, Phys. Rev. B43, 130 (1991).

[20] D. R. Nelson and V. M. Vinokur, Phys. Rev. Lett. 68, 2398 (1992).

[21] D. R. Nelson (private communications); see Appendix A in D. R. Nelson and V. M. Vinokur, Phys. Rev. B (1993) (in-press).

Figure Captions

Fig. 1. Temperature dependence of the resistivity of an untwinned $YBa_2Cu_3O_{7-\delta}$ single crystal for H | | c and H | | ab.

Fig. 2. Field dependence of the resistivity showing the hysteresis at B_m.

Fig. 3. H-T phase diagram for H | | c and H | | ab.

Fig. 4. Angular dependence of the melting temperature T_m for H=1.5 Tesla.

Fig. 5. Resistivity versus temperature at H=4T | | c for a single twin boundary crystal. Inset shows the effect of twin boundary pinning for magnetic field tilted about the c-axis.

Fig. 6. Resistivity versus temperature at H=6T | | c for a crystal with six twin boundaries. Inset shows the effect of six twin boundary pinning as a function of magnetic field tilted about the c-axis.

Fig. 7 Field dependence of the resistivity for T=79.01K and $\theta=1.2^o$, showing hysteretic behavior at the vortex melting field B_m.

Fig. 8. Temperature dependence of the resistivity before and after electron irradiation on an untwinned single crystal of $YBa_2Cu_3O_{7-\delta}$. The arrow shows the vortex melting temperature before irradiation.

Fig. 9. Voltage-current characteristics before and after electron irradiation at several different reduced temperatures T/T_c for H | | c.

Fig. 10. Resistivity versus temperature for H=8T at several angles tilted from the ab plane of the crystal.

Fig. 11. Plot of $1/[(1/\rho)(d\rho/dT)]$ versus T to determine T^* and s for H | | ab. The solid line is a linear least squares fit to the data between T_m=90.7K and 91.5K.

Fig. 12. Plot of H | | ab versus T^* and (Inset) the field dependence of the dynamic scaling exponent s obtained from figure 11.

Table 1

Sample characteristics

	T_c	ΔT_c	Characteristics
Crystal A	92.96	200mK	untwinned
Crystal B	92.66	220mK	one twin boundary
Crystal C	92.68	300mK	six twin boundary
Crystal D	93.16	300mK	untwinned/e-irradiated

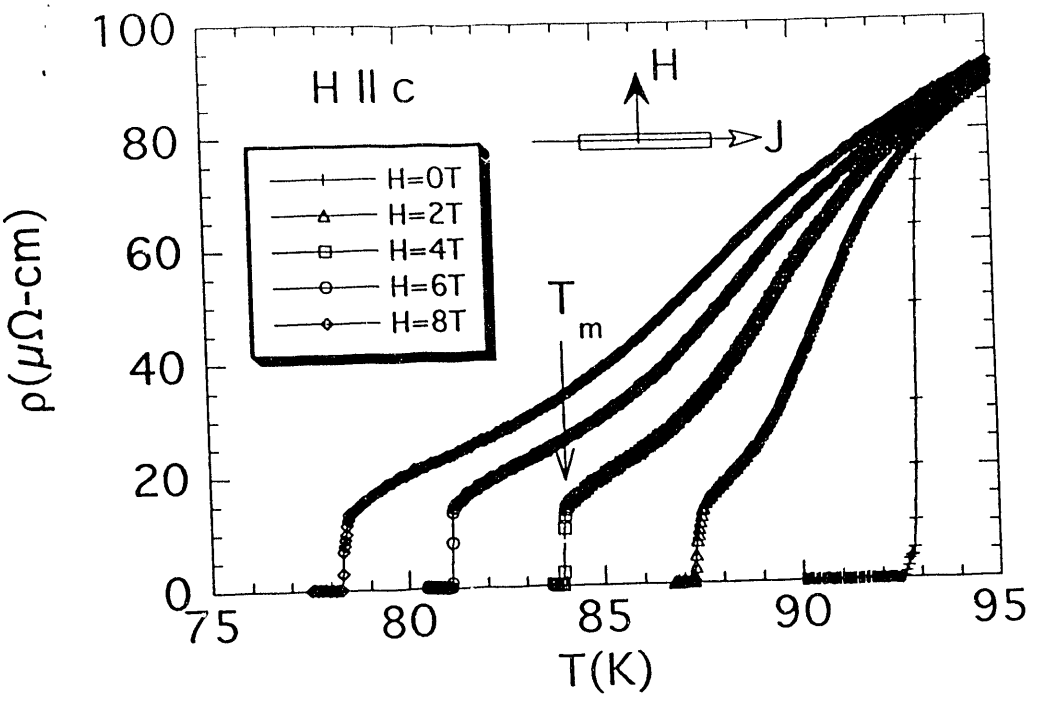
H ll c
H
J
H=0T
H=2T
H=4T
H=6T
H=8T
T m
ρ(μΩ-cm)
T(K)
100
80
60
40
20
0
75
80
85
90
95

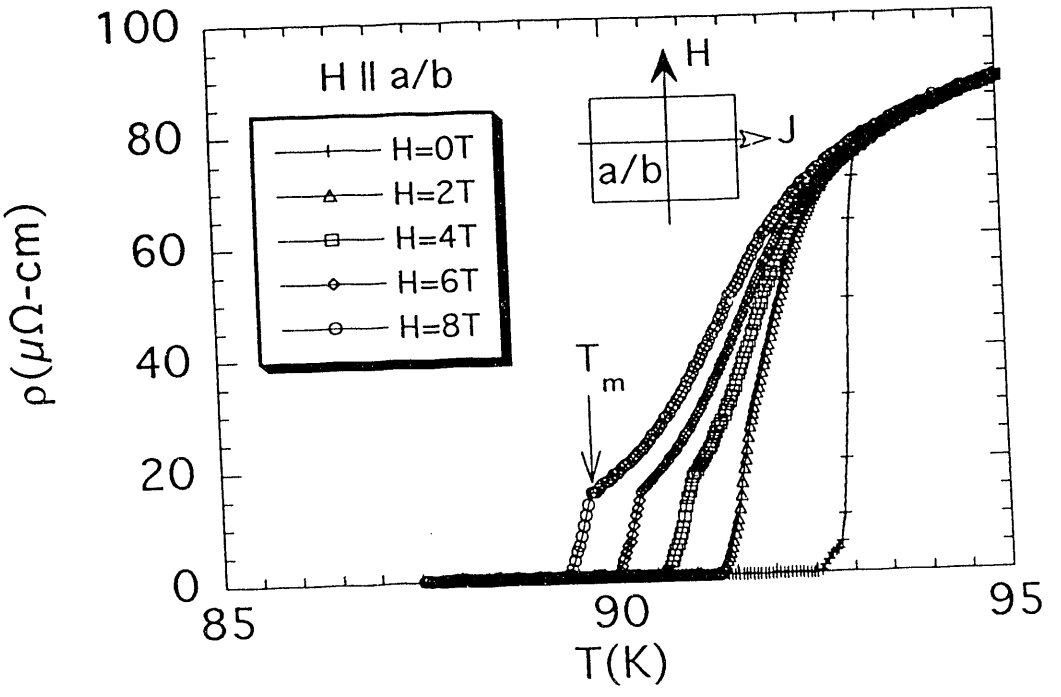
H ll a/b
H
J
a/b
H=0T
H=2T
H=4T
H=6T
H=8T
T m
ρ(μΩ-cm)
T(K)
100
80
60
40
20
0
85
90
95

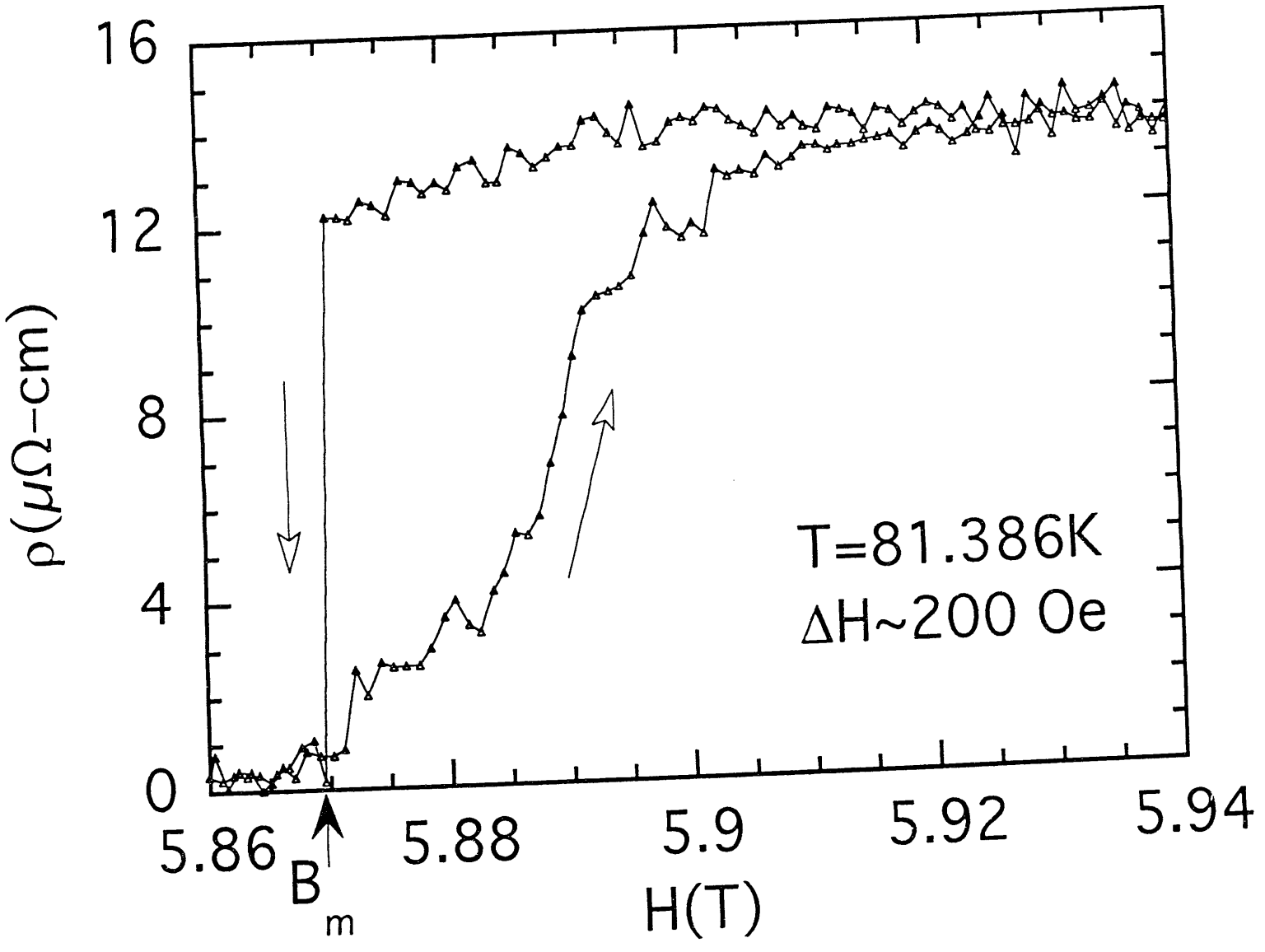
16
12
8
4
0
ρ(μΩ-cm)
5.86
5.88
5.9
5.92
5.94
H(T)
B
m
T=81.386K
ΔH~200 Oe

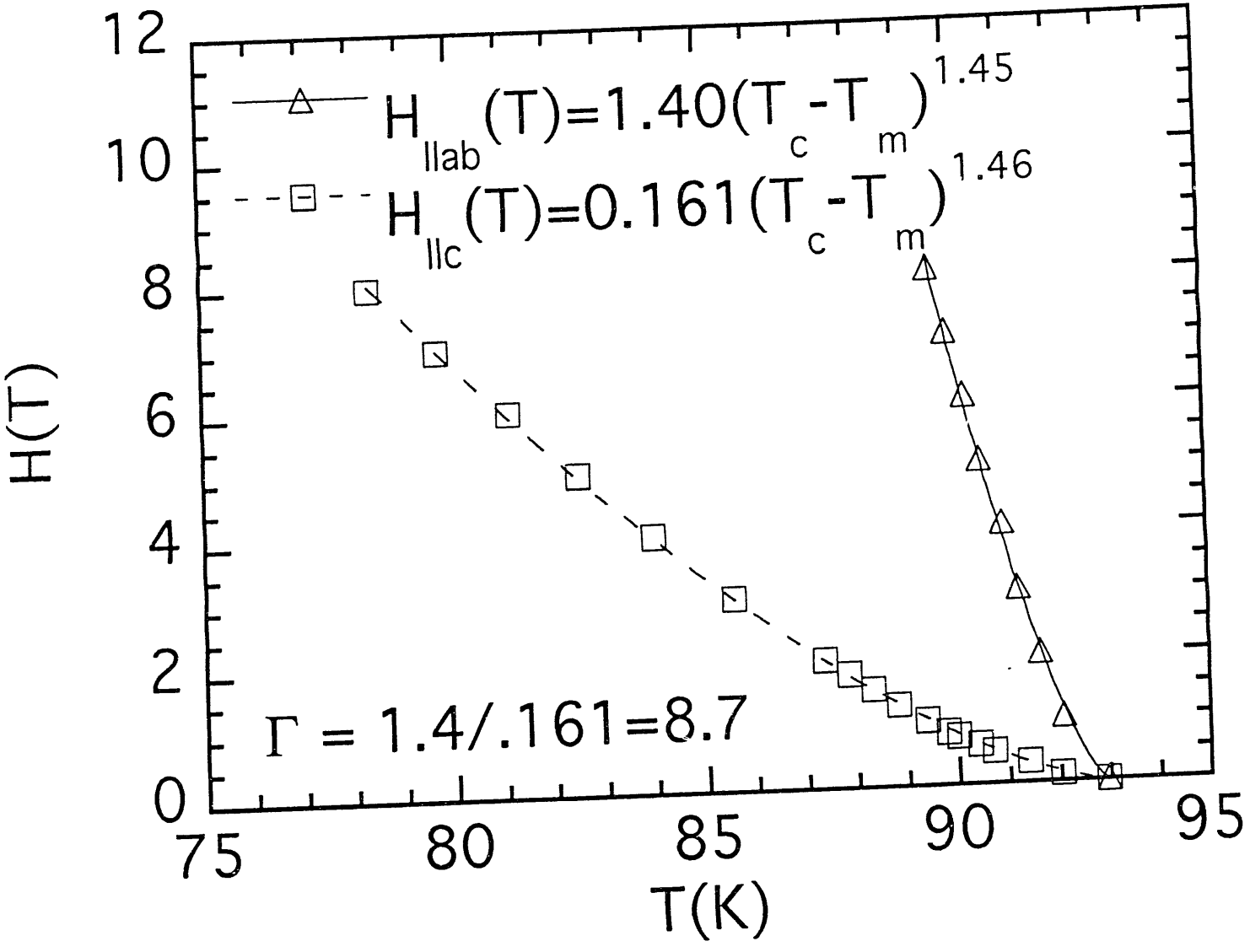
12
10
8
6
4
2
0
H(T)
75
80
85
90
95
T(K)
$H_{\parallel ab}(T)=1.40(T_c-T_m)^{1.45}$
$H_{\parallel c}(T)=0.161(T_c-T_m)^{1.46}$
$\Gamma = 1.4/.161=8.7$

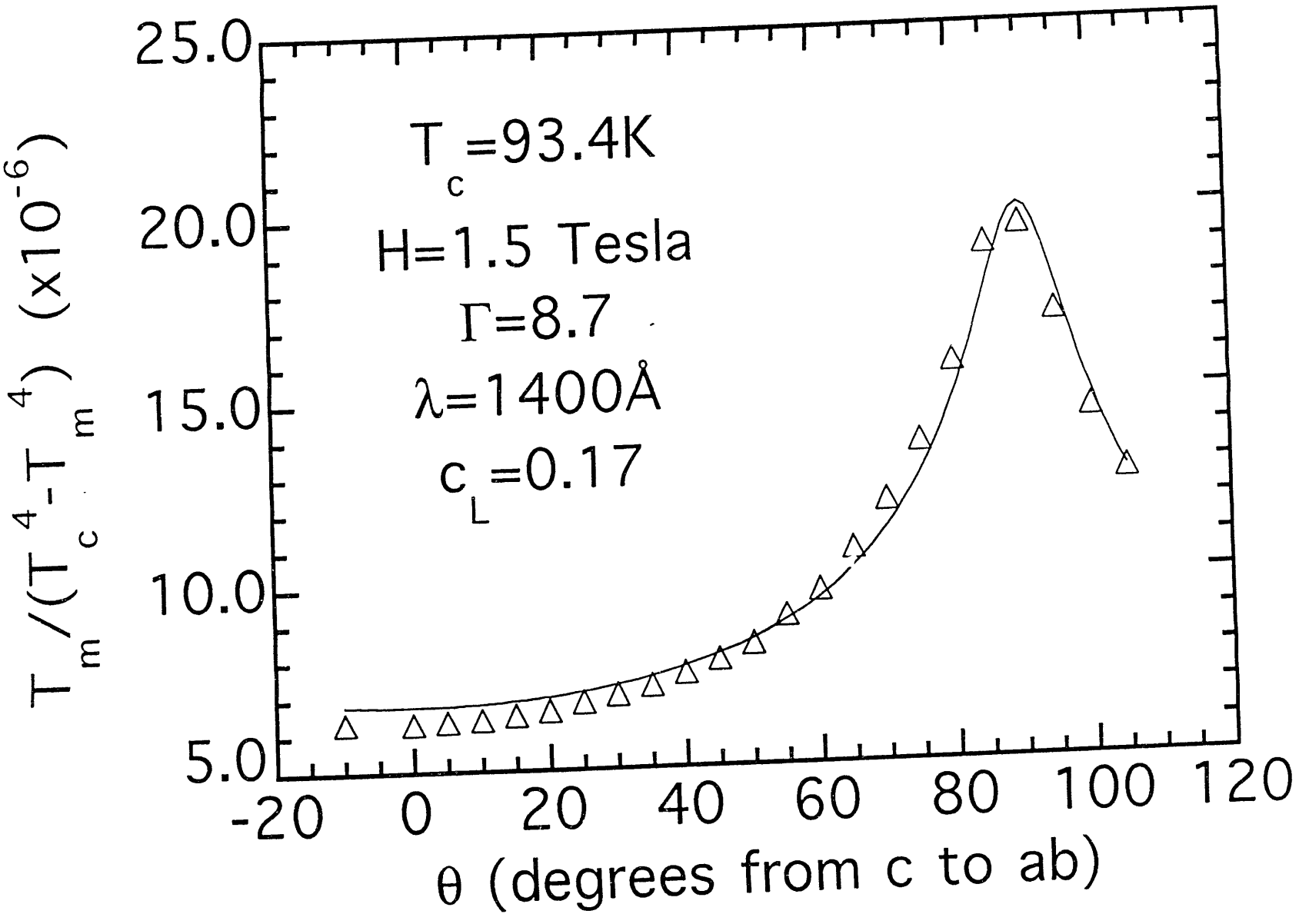
25.0
20.0
15.0
10.0
5.0
$T_m/(T_c^4-T_m^4)$ (x10^{-6})
T_c=93.4K
H=1.5 Tesla
Γ=8.7
λ=1400Å
c_L=0.17
-20
0
20
40
60
80
100
120
θ (degrees from c to ab)

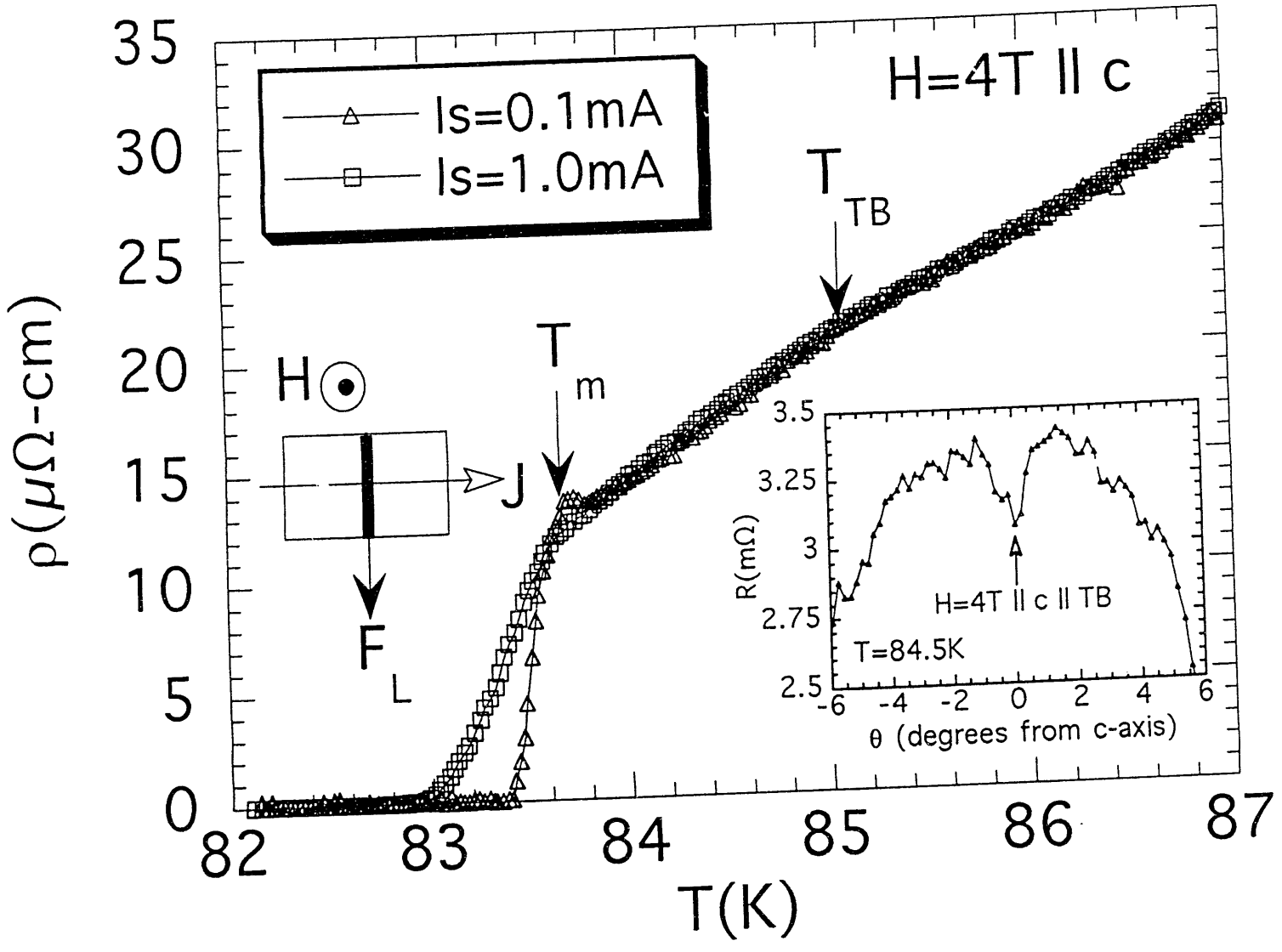
H=4T ll c
Is=0.1mA
Is=1.0mA
T
TB
T
m
H
J
F
L
ρ(μΩ-cm)
T(K)
R(mΩ)
H=4T ll c ll TB
T=84.5K
θ (degrees from c-axis)

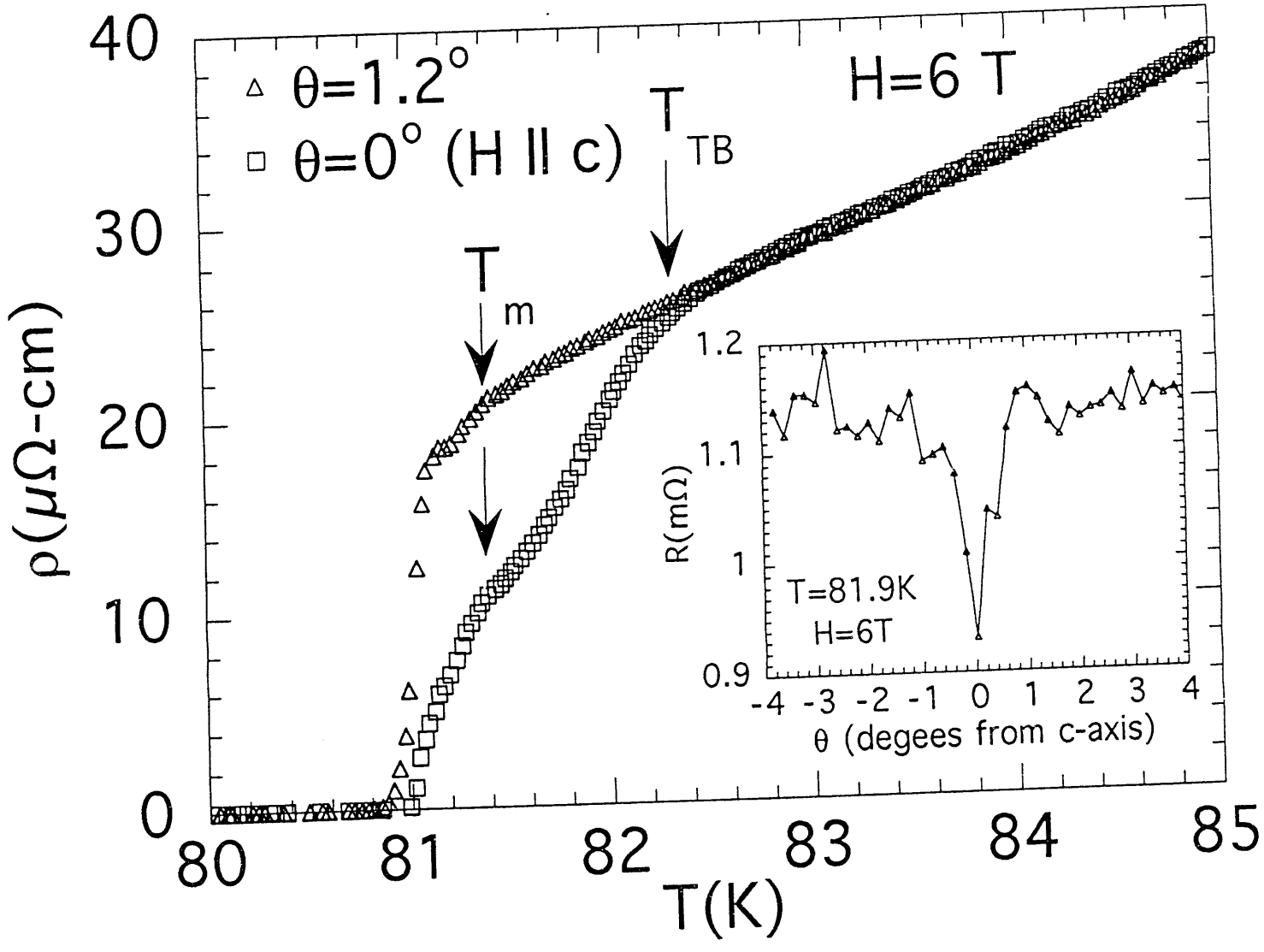
40
30
20
10
0
80
81
82
83
84
85
ρ(μΩ-cm)
T(K)
△ θ=1.2°
□ θ=0° (H ll c)
H=6 T
T TB
T m
1.2
1.1
1
0.9
R(mΩ)
T=81.9K
H=6T
-4 -3 -2 -1 0 1 2 3 4
θ (degees from c-axis)

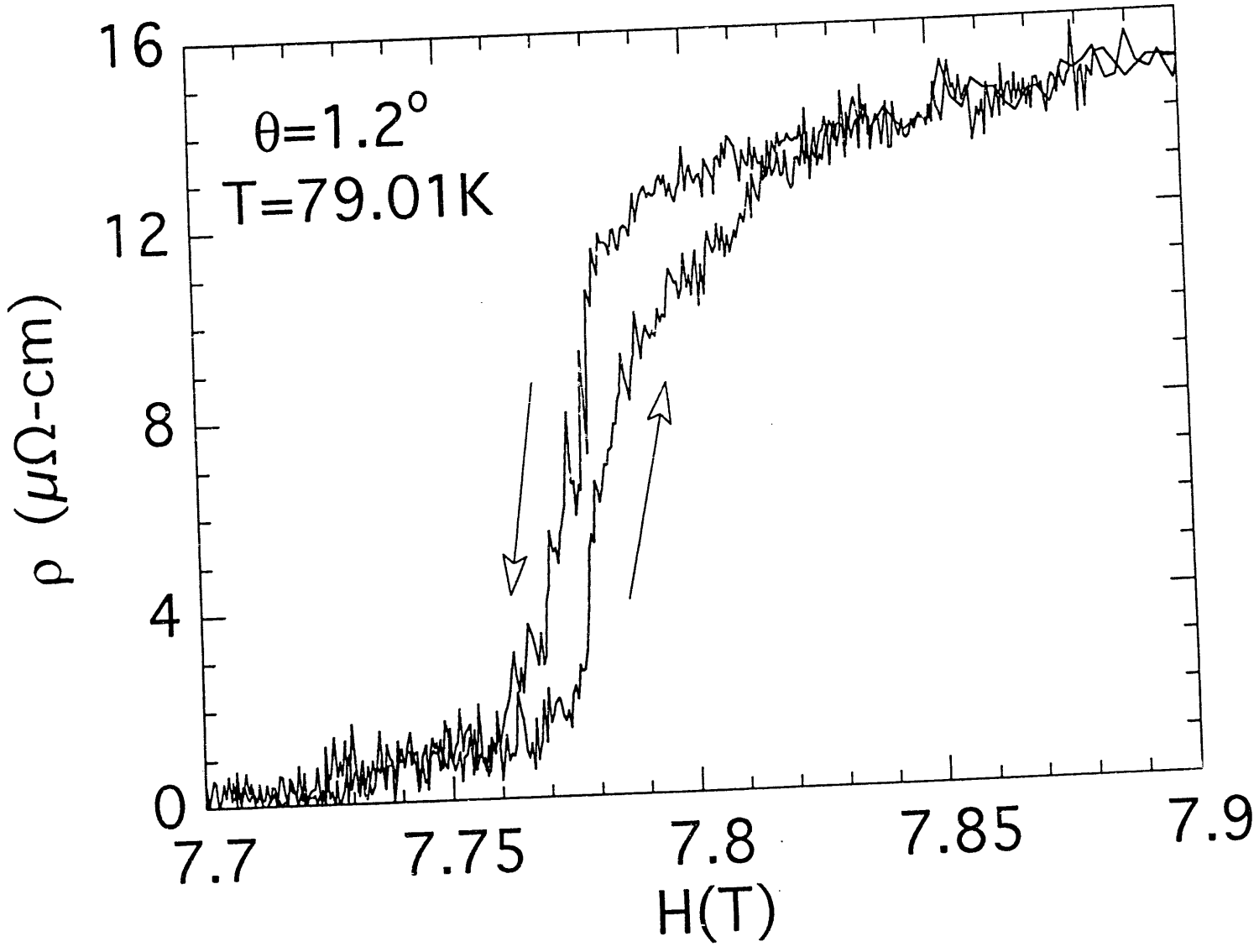
θ=1.2°
T=79.01K
ρ (μΩ-cm)
16
12
8
4
0
7.7
7.75
7.8
7.85
7.9
H(T)

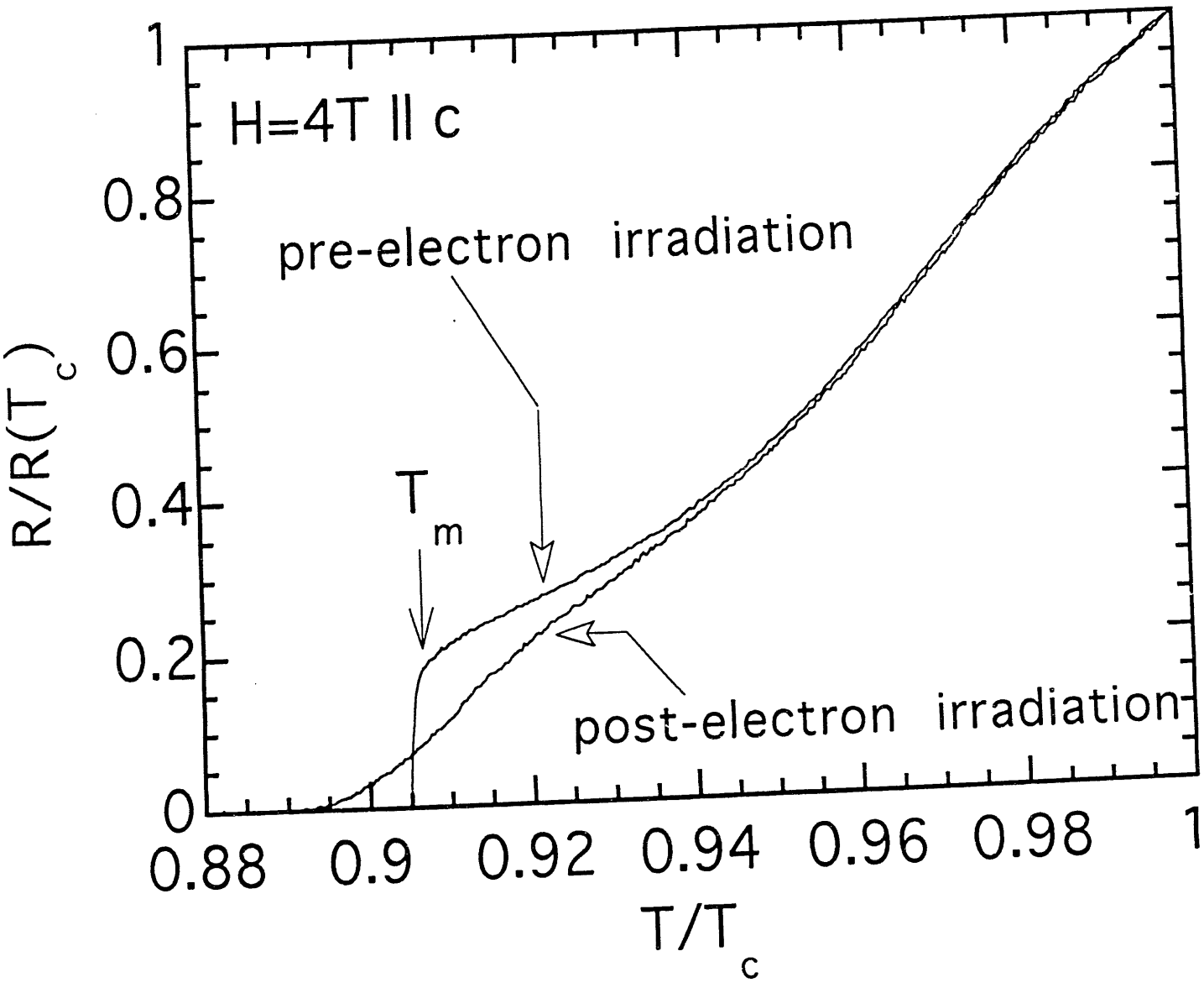
H=4T ll c
pre-electron irradiation
post-electron irradiation
T m
R/R(T c)
T/T c
0
0.2
0.4
0.6
0.8
1
0.88
0.9
0.92
0.94
0.96
0.98
1

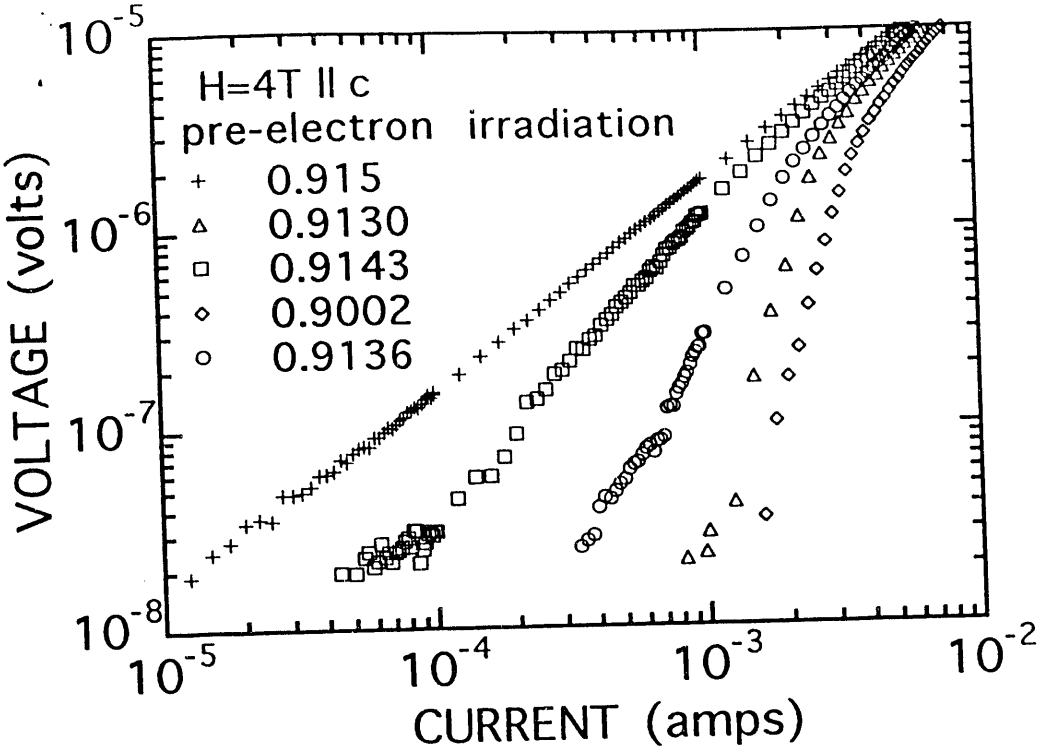
H=4T ll c
pre-electron irradiation
0.915
0.9130
0.9143
0.9002
0.9136
VOLTAGE (volts)
CURRENT (amps)
10^{-5}
10^{-6}
10^{-7}
10^{-8}
10^{-5}
10^{-4}
10^{-3}
10^{-2}

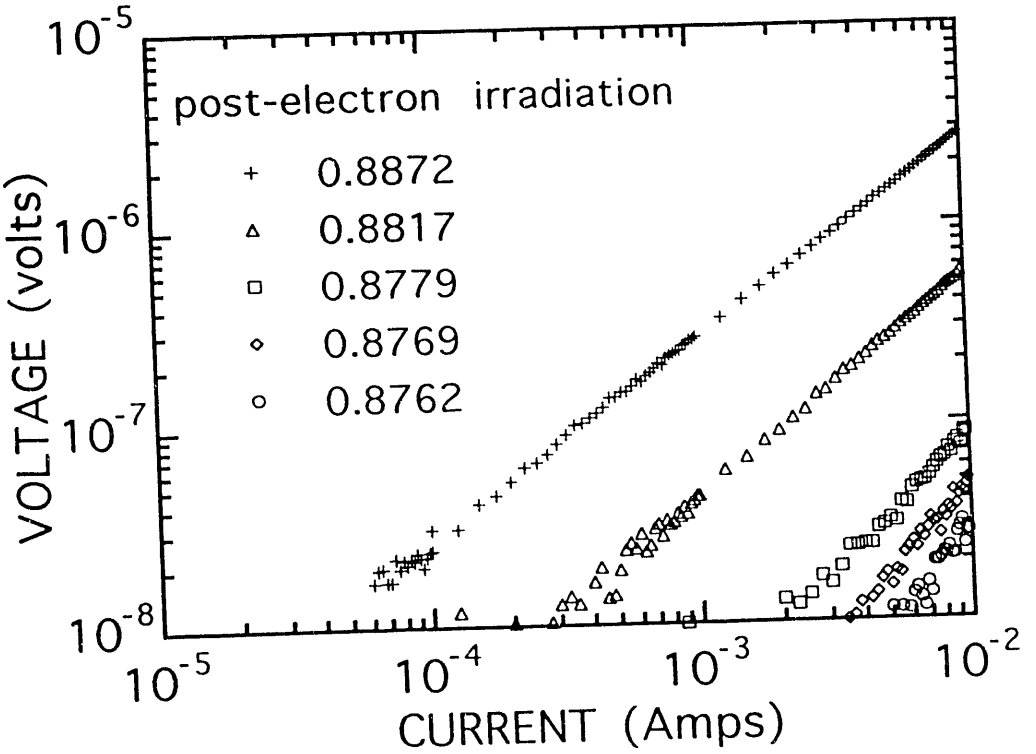
post-electron irradiation
0.8872
0.8817
0.8779
0.8769
0.8762
VOLTAGE (volts)
CURRENT (Amps)
10^{-5}
10^{-6}
10^{-7}
10^{-8}
10^{-5}
10^{-4}
10^{-3}
10^{-2}

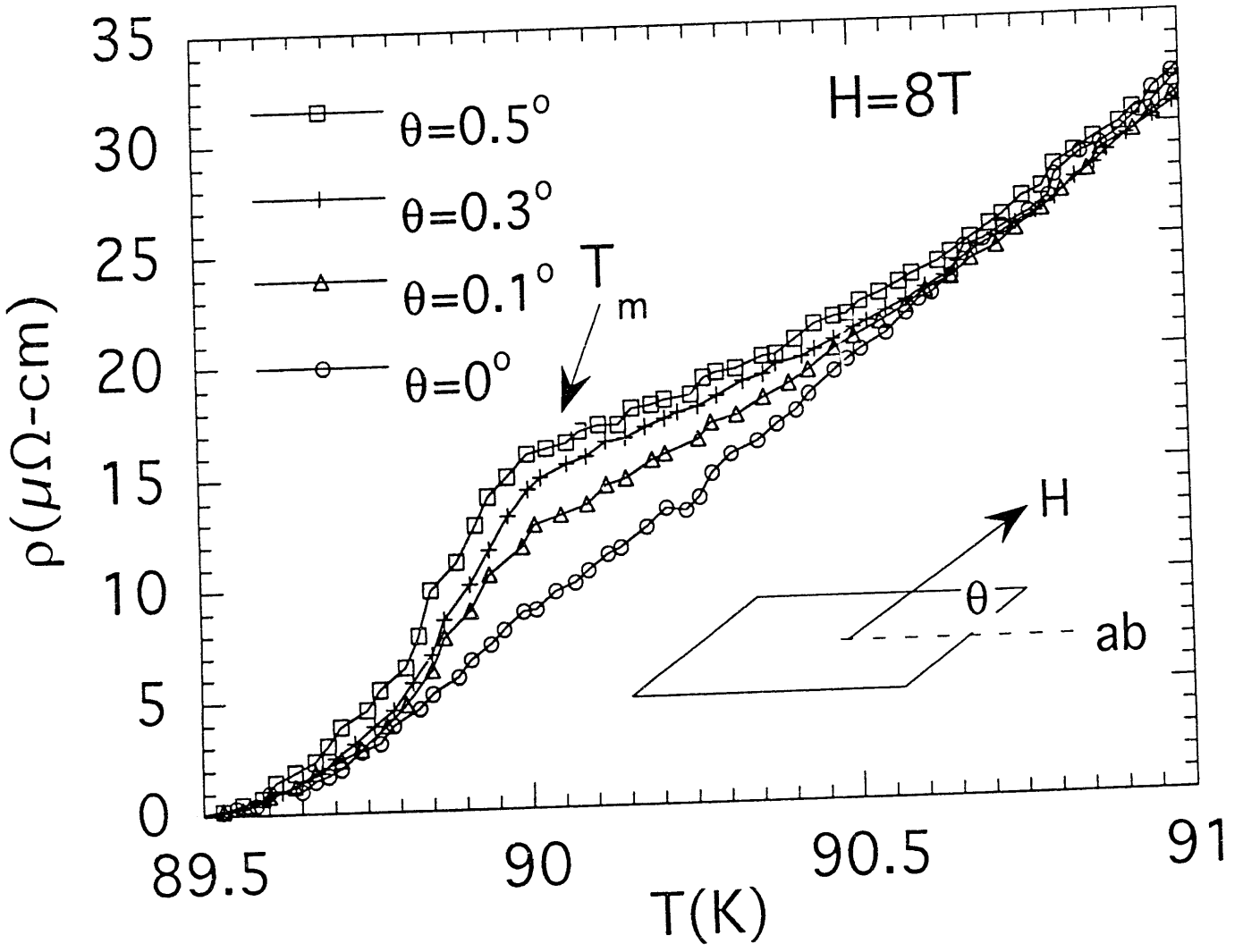
H=8T
θ=0.5°
θ=0.3°
θ=0.1°
θ=0°
T
m
H
θ
ab
ρ(μΩ-cm)
T(K)
0
5
10
15
20
25
30
35
89.5
90
90.5
91

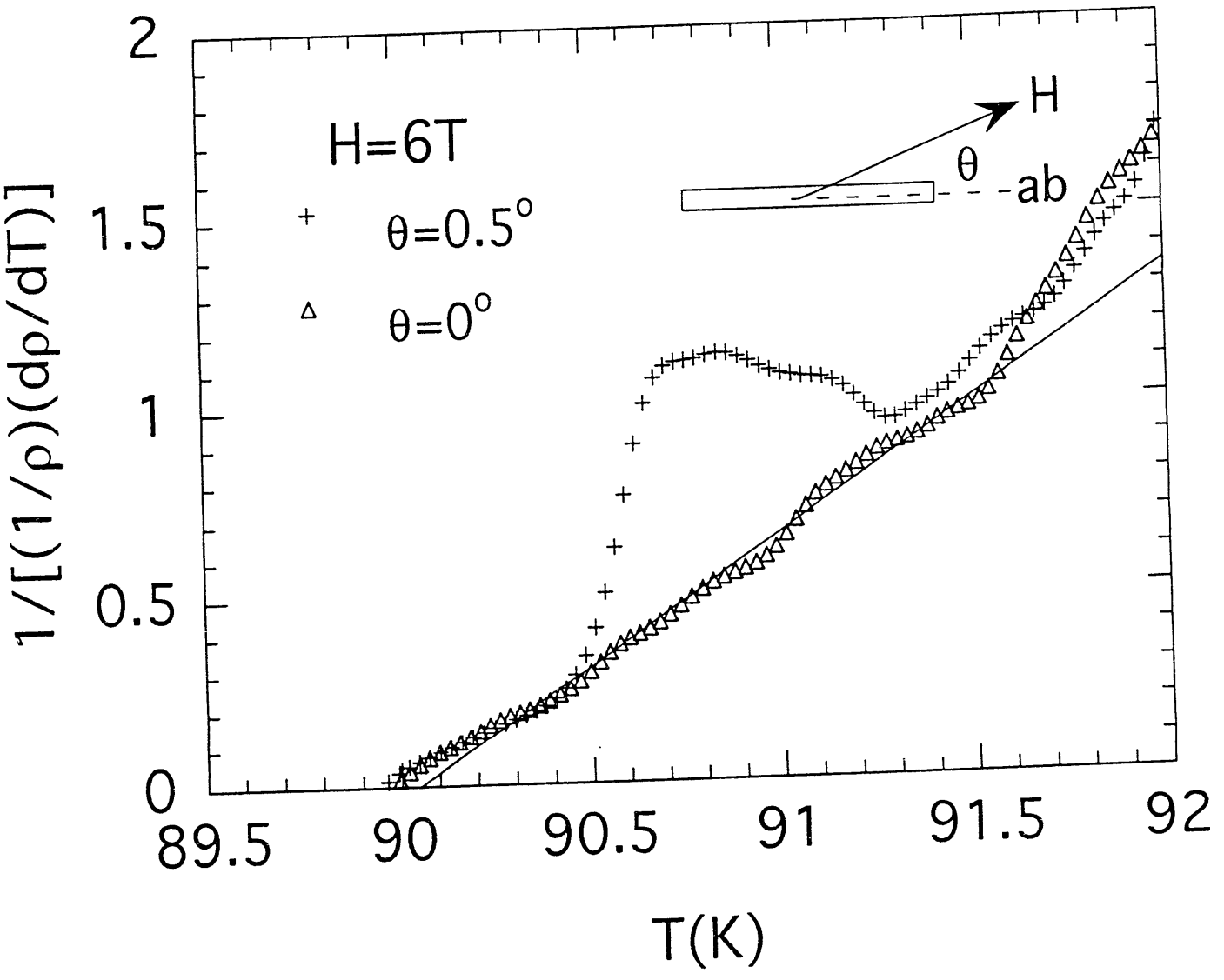
H=6T
θ=0.5°
θ=0°
H
θ
ab
1/[(1/ρ)(dρ/dT)]
T(K)
0
0.5
1
1.5
2
89.5
90
90.5
91
91.5
92

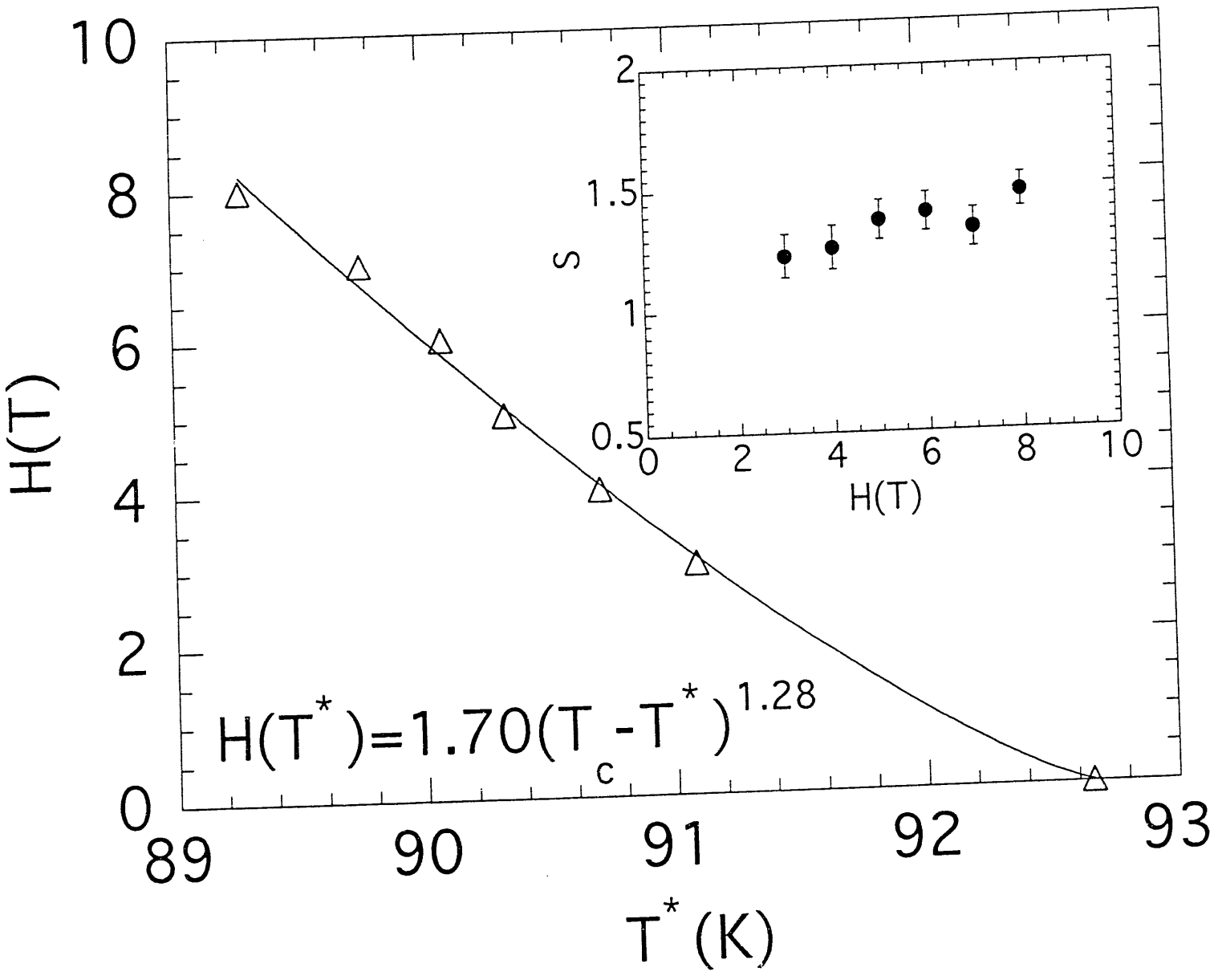
10
8
6
4
2
0
89
90
91
92
93
H(T)
T* (K)
H(T*)=1.70(Tc-T*)1.28
2
1.5
1
0.5
S
0
2
4
6
8
10
H(T)

DATE

FILMED

11/19/93

END